

# Magnetically tunable negative permeability metamaterial composed by split ring resonators and ferrite rods

Lei Kang, Qian Zhao, Hongjie Zhao, and Ji Zhou

State Key Laboratory of New Ceramics and Fine Processing, Department of Materials Science and Engineering,  
Tsinghua University, Beijing 100084, People's Republic of China  
[zhouji@mail.tsinghua.edu.cn](mailto:zhouji@mail.tsinghua.edu.cn)

**Abstract:** We experimentally demonstrate a tunable negative permeability metamaterial (NPM) at microwave frequencies by introducing yttrium iron garnet (YIG) rods into a periodic array of split ring resonators (SRRs). Different from those tuned by controlling the capacitance of equivalent LC circuit of SRR, this metamaterial is based on a mechanism of magnetically tuning the inductance via the active ambient effective permeability. For magnetic fields from 0 to 2000 Oe and from 3200 to 6000 Oe, the resonance frequencies of the metamaterial can blueshift about 350 MHz and redshift about 315 MHz, respectively. Both shifts are completely continuous and reversible. Correspondingly, the tunable negative permeabilities are widened by about 360 MHz and 200 MHz compared to that without YIG rods.

© 2008 Optical Society of America

OCIS codes: (999.9999) Metamaterials; (350.4010) Microwaves.

---

## References and links

1. J. B. Pendry, "Negative refraction makes a perfect lens," *Phys. Rev. Lett.* **85**, 3966-3969 (2000).
2. R. A. Shelby, D. R. Smith, and S. Schultz, "Experimental verification of a negative index of refraction," *Science* **292**, 77-79 (2001).
3. D. R. Smith, W. J. Padilla, D. C. Vier, S. C. Nemat-Nasser, and S. Schultz, "Composite medium with simultaneously negative permeability and permittivity," *Phys. Rev. Lett.* **84**, 4184-4187 (2000).
4. A. Houck, J. B. Brock, and I. L. Chuang, "Experimental observations of a left-handed material that obeys Snell's law," *Phys. Rev. Lett.* **90**, 137401 (2003).
5. C. G. Parazzoli, R. B. Gregor, K. Li, B. E. C. Koltenbah, and M. Tanielian, "Experimental verification and simulation of negative index of refraction using Snell's law," *Phys. Rev. Lett.* **90**, 107401 (2003).
6. N. Seddon and T. Bearpark, "Observation of the inverse Doppler effect," *Science* **302**, 1537-1540 (2003).
7. V. G. Veselago, "The electrodynamics of substances with simultaneously negative values of  $\epsilon$  and  $\mu$ ," *Soviet Physics USPEKI* **10**, 509-514 (1968).
8. J. B. Pendry, A. J. Holden, D. J. Robbins, and W. J. Steward, "Magnetism from conductors and enhanced nonlinear phenomena," *IEEE Trans. Microwave Theory Tech.* **47**, 2075-2084 (1999).
9. J. B. Pendry, A. J. Holden, D. J. Robbins, and W. J. Steward, "Low frequency plasmons in thin-wire structures," *J. Phys. Condens. Matter* **10**, 4785-4808 (1998).
10. D. Schurig, J. J. Mock, B. J. Justice, S. A. Cummer, J. B. Pendry, A. F. Starr, and D. R. Smith, "Metamaterial electromagnetic cloak at microwave frequencies," *Science* **314**, 977-980 (2006).
11. W. Cai, U. Chettiar, A. V. Kildishev, and V. M. Shalaev, "Optical cloaking with metamaterials," *Nature Photonics* **1**, 224-227 (2007).
12. F. J. Rachford, D. N. Armstead, V. G. Harris and C. Vittoria, "Simulations of ferrite-dielectric-wire composite negative index materials," *Phys. Rev. Lett.* **99**, 057202 (2007).
13. A. Pimenov, A. Loid, K. Gehrke, V. Moshnyaga, and K. Samwer, "Negative refraction observed in a metallic ferromagnet in the gigahertz frequency range," *Phys. Rev. Lett.* **98**, 197401 (2007).
14. H. J. Zhao, J. Zhou, Q. Zhao, B. Li, L. Kang, and Y. Bai, "Magnetically tunable left-handed material consisting of yttrium iron garnet slab and metallic wires," *Appl. Phys. Lett.* **91**, 131107 (2007).

15. B. Hou, G. Xu, H. K. Wong, and W. J. Wen, "Tuning of photonic bandgaps by a field-induced structural change of fractal metamaterials," *Opt. Express* **13**, 9149-9154 (2005).
16. W. J. Padilla, A. J. Taylor, C. Highstrete, M. Lee, and R. D. Averitt, "Dynamical electric and magnetic metamaterial response at terahertz frequencies," *Phys. Rev. Lett.* **96**, 107401 (2006).
17. X. P. Zhao, Q. Zhao, L. Kang, J. Song, and Q. H. Fu, "Defect effect of split ring resonators in left-handed metamaterials," *Phys. Lett. A* **346**, 87-91 (2005).
18. H. T. Chen, W. J. Padilla, J. M. O. Zide, A. C. Gossard, A. J. Taylor, and R. D. Averitt, "Active terahertz metamaterial devices," *Nature* **444**, 597-600 (2006).
19. I. Gil, J. G. Garcia, J. Bonache, F. Martin, M. Sorolla, and R. Marques, "Varactor-loaded split ring resonators for tunable notch filters at microwave frequencies," *Electron. Lett.* **40**, 1347-1348 (2004).
20. H. Chen, Bae-Ian Wu, L. Ran, T. M. Grzegorzczuk, and J. A. Kong, "Controllable left-handed metamaterial and its application to a steerable antenna," *Appl. Phys. Lett.* **89**, 053509 (2006).
21. I. V. Shadrivov, S. K. Morrison, and Y. S. Kivshar, "Tunable split-ring resonators for nonlinear negative-index metamaterials," *Opt. Express* **14**, 9344-9349 (2006).
22. Q. Zhao, L. Kang, B. Du, B. Li, and J. Zhou, "Electrically tunable negative permeability metamaterials based on nematic liquid crystals," *Appl. Phys. Lett.* **90**, 011112 (2007).
23. D. H. Werner, Do-Hoon Kwon, and Iam-Choon Khoo, "Liquid crystal clad near-infrared metamaterials with tunable negative-zero-positive refractive indices," *Opt. Express* **15**, 3342-3347 (2007).
24. A. Degiron, J. J. Mock, and D. R. Smith, "Modulating and tuning the response of metamaterials at the unit cell level," *Opt. Express* **15**, 1115-1127 (2007).
25. E. Ozbay, K. Aydin, S. Butun, K. Kolodziejek, and D. Pawlak, "Ferroelectric based tuneable SRR based metamaterial for microwave applications," in *Proceedings of the 37th European Microwave Conference* (Institute of Electrical and Electronics Engineers, New York, 2007), pp. 497-499.
26. W. A. Roshen, "Effect of Finite Thickness of Magnetic Substrate on Planar Inductors," *IEEE Trans. Magn.* **26**, 270-275 (1990).
27. K. Shirakawa, S. Ishibashi, Y. Kobayashi, F. Takeda, and K. Murakami, "A new planar inductor with ring-connected magnetic core," *IEEE Trans. Magn.* **26**, 2268-2270 (1990).
28. X. Y. Gao, Y. Zhou, Y. Cao, C. Lei, W. Ding, H. Choi, and J. Won, "A copper/polyimide fabrication process for fabricating high-inductance microinductor," *IEEE Trans. Elec. Pack. & Manu.* **30**, 123-127 (2007)
29. B. Lax and K. J. Button, *Microwave ferrites and ferrimagnetics*, (McGraw-Hill, New York, 1962).
30. V. B. Bregara and M. Pavlin, "Effective-susceptibility tensor for a composite with ferromagnetic inclusions: enhancement of effective-media theory and alternative ferromagnetic approach," *J. Appl. Phys.* **95**, 6289-6293 (2004).
31. V. B. Bregara, "Effective-medium approach to the magnetic susceptibility of composites with ferromagnetic inclusions," *Phys. Rev. B* **71**, 174418 (2005).
32. G. W. Milton, "Bounds on the complex permittivity of a two-component composite material," *J. Appl. Phys.* **52**, 5286-5293 (1981).
33. A. M. Nicholson and G. F. Ross, "Measurement of the intrinsic properties of materials by time domain techniques," *IEEE Trans. Instrum. Meas.* **19**, 377-382 (1970).
34. D. R. Smith, D. C. Vier, Th. Koschny, and C. M. Soukoulis, "Electromagnetic parameter retrieval from inhomogeneous metamaterials," *Phys. Rev. E* **71**, 036617 (2005).
35. O. Reynet and O. Acher, "Voltage controlled metamaterial," *Appl. Phys. Lett.* **84**, 1198-1200 (2004).

## 1. Introduction

Left-handed metamaterials (LHMs) have been investigated intensely [1-6] for their novel properties never existed in natural materials, especially the subwavelength resolving power of electromagnetic wave [1]. These properties are attributed to both negative permittivity and permeability, originally proposed by Veselago [7] and experimentally verified by Shelby, *et al.* [2] through negative refraction in a prism composed of a periodic array of split ring resonators (SRRs) and wires with Pendry's models [8, 9]. Recently, the investigations of electromagnetic cloak of invisibility based on the refractive index design of metamaterial in both microwave [10] and optical frequency ranges [11] have generated great interests. However, most metamaterials proposed to date are based on immutable structure of the unit cell, which results in a rather narrow band or even single frequency where the cloak is well functioned, and thus a highly limited practicability. It should be noted that, not only for the electromagnetic cloak but also for all the further applications theoretically promised, tunability

is certainly crucial for metamaterials. Fortunately, various efforts have been devoted to achieve tunability.

On the one hand, another approach to constructing metamaterials without metallic structures has been reported recently, that is, through the resonance of the natural materials to obtain the negative effective parameters [12, 13]. An advantage of this kind of metamaterials is their electromagnetic properties could be easily tuned by temperature, electric or magnetic field, etc [12-14]. Nevertheless, the resonance is strictly limited by the intrinsic properties of these materials which could not be designed at will theoretically.

On the other hand, tunable metamaterials could also be achieved by controlling the dielectric or magnetic properties of ambient of structure units [15-18]. An ideal split ring resonator (SRR) can be regarded as a LC circuit whose resonance is determined by the effective inductance L and the effective capacitance C, and its resonance frequency is given by  $\omega = 1/\sqrt{LC}$ . By inserting varactors into the structures, Gil *et al.* [19] and Chen *et al.* [20] have simulated the electrically controlled metamaterial. Shadrivov *et al.* [21] have demonstrated the tunability of the varactor-loaded split-ring resonator structures based on self-induced nonlinear effects at relatively low power levels. Zhao *et al.* [22] have reported the electrically tunable properties of negative permeability metamaterial (NPM) composed by an array of SRRs immersed in nematic liquid crystals (NLCs) by changing the orientation of LC. Werner *et al.* [23] have shown liquid crystal clad near-infrared metamaterials with tunable negative-zero-positive refractive indices. Degiron *et al.* [24] have demonstrated the modulating response of unit SRR by illuminating the low doped silicon positioned within the gap with infrared laser. And Ozbay *et al.* [25] have investigated the active response of SRRs by varying the dielectric permittivity of ferroelectric film deposited on the substrate with the temperature.

Nevertheless, the above mentioned tunability in metamaterials is mainly derived from the capacitance control of equivalent LC circuit of SRR by electric field. There are still few reports on the control of inductance to achieve similar tuning effects on the resonance of SRR by magnetic field. In this paper, by introducing yttrium iron garnet (YIG) ferrite rods into the ambient of a period array of SRRs, we propose and experimentally demonstrate a magnetically tunable negative permeability metamaterial. In addition, a qualitative explanation has also been suggested based on the effective-medium theory.

## 2. Approach to tunability

Similar to the correlation between capacitance C and permittivity  $\epsilon$ , inductance L of LC circuits could be expressed as a function of ambient effective permeability  $\bar{\mu}_{am}$  [26-28], i.e.,  $L \propto \bar{\mu}_{am} = \mu_1 + i\mu_2$ , where  $\mu_1$  and  $\mu_2$  are real and imaginary parts, respectively determining the corresponding part of inductance L. As a result, based on equation  $\omega = 1/\sqrt{LC}$ , the resonance frequency of NPM can be tuned by altering  $\bar{\mu}_{am}$ , i.e., the resonance frequency would decrease with increasing  $\mu_1$  and vice versa. On the other hand, an actual SRR is equal to a LRC circuit, where R, i.e., effective resistance represents the inevitable dissipation and determines the damping exponential of the resonance. It has been known that the imaginary part of inductance L can be regarded as a part of the effective resistance of the circuit. Therefore, the resonance strength will decrease with  $\mu_2$  and, for  $\mu_2$  of a certain large value, negative permeability of the metamaterial composed of SRRs would not be encountered because of the damped resonance.

## 3. Experiments

In this section, we experimentally demonstrate a magnetically tunable NPM by introducing magnetic materials with controllable permeability under direct current (dc) magnetic field.

The NPM used here (see Fig. 1) is composed of a periodic array of copper SRRs, which were fabricated by a shadow mask/etching technique on a 0.9 mm thick substrate with a permittivity of 3.3. The lattice constant of the resulted metamaterial is 5 mm. The dimensions of SRRs are  $d_1=0.80$  mm,  $d_2=1.80$  mm,  $c=0.20$  mm,  $g=0.40$  mm, and the thickness  $t=0.03$  mm.

Magnetic materials exhibiting strong magnetic responses at GHz are relatively rare, i.e., most of them have unity permeability in this frequency range, whether the magnetic field is applied or not. Yttrium iron garnet (YIG), a commercially available ferrite, has been chosen here for its strong dispersion of permeability due to its magnetically controllable ferromagnetic resonance (FMR) over a broad microwave frequency range [29]. Saturation magnetization, linewidth and permittivity of the used YIG, which determine the magnetic permeability response of the ferrite under magnetic field, are 1700 Gs, 12 Oe and constant 14.7, respectively. With side length of 0.8 mm, which is significantly smaller than the wavelength of the microwave magnetic field, the square-sectioned YIG rods are placed at the symmetry axes of SRRs as Fig. 1 shows.

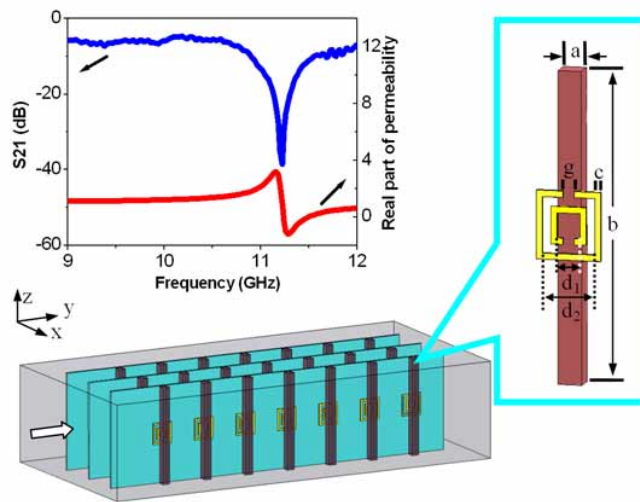


Fig. 1. Schematic of the magnetically tunable negative permeability metamaterial (NPM) composed of SRRs and YIG rods. Electromagnetic wave with magnetic field polarized along the x direction propagates along the y axis. External dc magnetic fields ( $\mathbf{H}_0$ ) are applied along the z axis. Dependence of S21 parameter and effective permeability of sole NPM without YIG rods on frequency are shown in the upper inset.

Based on the coordinate system shown in Fig. 1, in the presence of external dc magnetic fields ( $\mathbf{H}_0$ ) along the z axis, the permeability of YIG rods would be a tensor with the dispersive element  $\bar{\mu}_{x,YIG\ rod}$  which corresponds to the direction of microwave magnetic field and the non-dispersive elements  $\bar{\mu}_{y,YIG\ rod} = \bar{\mu}_{z,YIG\ rod} \rightarrow 1$  in which the imaginary parts could be ignored [12]. It is reasonable to expect that ambient effective permeability  $\bar{\mu}_{x,am} = \mu_{1x} + i\mu_{2x}$  ( $\bar{\mu}_{y,am}$  and  $\bar{\mu}_{z,am}$  would be unity) could be calculated with effective-medium theory [30, 31] due to the low space-filling factor ( $2.56 \times 10^{-2}$ ) of YIG rods and isotropic unity permeability of air. Nevertheless, it is impracticable to quantitatively analyze effective permeability of composites with rod-shape inclusions because the shape effect in homogenization is significant in effective-medium theory [32]. Fortunately, in accordance with Ref [31, 32], qualitative evolution of the dependence of effective permeability of magnetic effective medium on magnetic field would be analogous with that of the magnetic

components, despite the significant variation including shifting of the resonance frequency on account of the interaction among the magnetic components. Therefore, by calculating the dependence of permeability of single YIG rod on magnetic field (meanwhile taking into consideration of the shape demagnetizing effects) [29], we could qualitatively characterize the evolution of that of  $\bar{\mu}_{x,am}$  at the resonance frequency (10.71 GHz as detailedly discussed below) of NPM with YIG rods, as Fig. 2 shows. And the vertical axes have not been labeled accordingly. The validity of this presentation would be demonstrated by the experimental results below. In addition, according to the discussion in Section 2, the behavior of NPM sample would be determined by the variation of  $\bar{\mu}_{x,am}$ . We hereby divided Fig. 2 into three regimes based on the evolution: “low” magnetic field, where  $\bar{\mu}_{x,am}$  decreases from unity to lower values; “medium” magnetic field, where imaginary part of  $\bar{\mu}_{x,am}$  has been found to play a significant role; and “high” magnetic field, where  $\bar{\mu}_{x,am}$  decreases from higher values, toward unity.

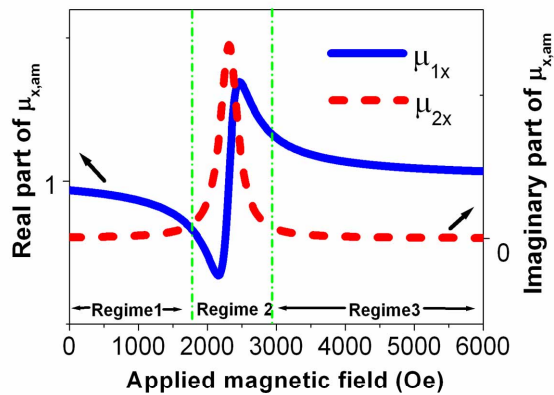


Fig. 2. Qualitative evolution of the dependence of  $\bar{\mu}_{x,am}$  on magnetic field based on calculation of that of single YIG rod [29]. Applied magnetic field is divided into three regimes of “low”, “medium” and “high” according to the evolution.

With the sample inserted into X-band rectangular waveguide WR90 with a cross section of  $22.86 \times 10.14 \text{ mm}^2$ , the scattering parameters are measured by an HP8720ES network analyzer. In the presence of external dc magnetic fields ( $\mathbf{H}_0$ ) along the z axis, the tunable transmission coefficient (the S21 parameter) normalized against the transmission of the unloaded waveguide can be easily obtained. We firstly measure the S21 parameters of a sole NPM sample without YIG rods. An invariable magnetic resonance emerges at 11.22 GHz (as indicated in the inset of Fig. 1) when dc magnetic fields in the range of concern are applied. Included also in the inset of Fig. 1 is the real part of effective permeability of the sole NPM sample which would be detailedly discussed below.

Based on the evolution of  $\bar{\mu}_{x,am}$  in Fig. 2, we divide the transmission experiments into three sections (shown in Fig. 4, Fig. 5 and Fig. 6, respectively) to clearly organize the documentation, meanwhile to create an opportunity for comparison among the results. In all the three figures, the solid curves represent the resonances under zero magnetic field. They indicate that the sample with YIG rods resonates at 10.71 GHz and the resonance frequency (the transmission dip) shifts about 0.5 GHz toward lower frequency compared to that of the sole NPM sample. This is attributed to the increase of ambient effective permittivity after introducing YIG rods.

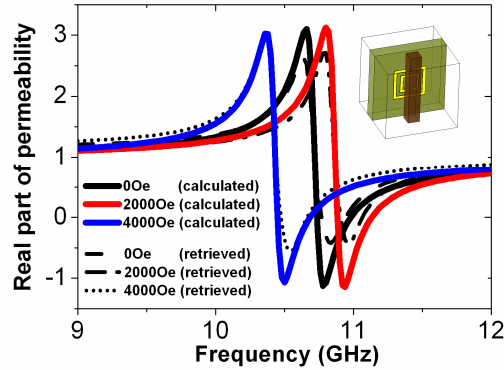


Fig. 3. Calculated and retrieved effective permeabilities (by Eq. (1) and retrieval procedure [33, 34] respectively) of the simulation model (NPM with YIG rods) under dc magnetic fields of 0, 2000 and 4000 Oe are shown. The inset shows the model of simulation.

In our experiment, because of the application of electromagnet, it turns out difficult to obtain a precise measurement of both of the transmission and reflection information by repeatedly assembling the waveguides and matching loads. Accordingly, the retrieval procedure discussed in Ref. [33, 34] has not been chosen. Alternatively, with known structure parameters and resonance frequency  $\omega_0$  determined by the structure and material, the effective permeability of the SRR-array metamaterial could be calculated according to the expression in Ref. [8],

$$\bar{\mu}_{meta}(\omega) = 1 - \frac{F\omega^2}{\omega^2 - \omega_0^2 + i\Gamma\omega} \quad (1)$$

where  $F$  is the fractional volume of the unit cell occupied by the interior of the SRRs and  $\Gamma$  is the dissipation factor. In our case, with a changeless structure of metamaterial, the resonance frequency  $\omega_0$ , which is indicated by the dip in the  $S_{21}$  curve measured under corresponding magnetic field, is substituted into Eq. (1) to obtain the effective permeability of the sample [22]. And  $F=0.05$  and  $\Gamma=10^{10}/4\pi$  have been selected for the designed metamaterial. It should be noted that, Eq. (1) was not deduced specifically for metamaterial containing magnetic materials, and the accurate expression would be much more complex [35]. With commercial software HFSS, we simulated the scattering parameters of the structure (for one unit cell length as that in Ref. [34], see the inset of Fig. 3) similar to that of our experiment under dc magnetic fields of 0, 2000 and 4000Oe. And then we obtained the effective permeabilities (plotted in Fig. 3) from Eq. (1) by substituting the resonance frequencies indicated by the simulated  $S$  parameters. In addition, we plotted the corresponding retrieved effective permeabilities obtained through the procedures discussed in Ref. [33, 34] for comparison. It can be seen from Fig. 3 that the calculated effective permeabilities accord well with the retrieved ones, demonstrably showing that Eq. (1) is an adequate approximation for metamaterials containing magnetic materials whose permeability is expected to be small.

Figure 4 shows the tuning resonances of NPM sample under “low” magnetic field within the range of 0 Oe to 2000 Oe. In Fig. 4(a), where the corresponding  $S_{21}$  parameters are shown, the magnetic resonance frequency of NPM shifts continuously from 10.71 GHz to 11.06 GHz with increasing magnetic fields. Comparison of the shift of  $H_0=1000$  Oe with that of  $H_0=2000$  Oe indicates an accelerated resonance frequency blueshift of NPM. Additionally, Fig. 4(a) also reveals the almost invariable amplitude during the whole process. According to the discussion in section 2, the tuning of NPM’s magnetic resonance originates from the

altered  $\bar{\mu}_{x,am}$  under dc magnetic field. Fig. 2 shows that, with magnetic field increasing in range of regime 1,  $\mu_{1x}$ , the real part of  $\bar{\mu}_{x,am}$  decreases with increasing slope, while  $\mu_{2x}$ , the imaginary part approximates to zero and shows little change on the whole. This indicates the correspondence between the experimental results and theoretical predictions.

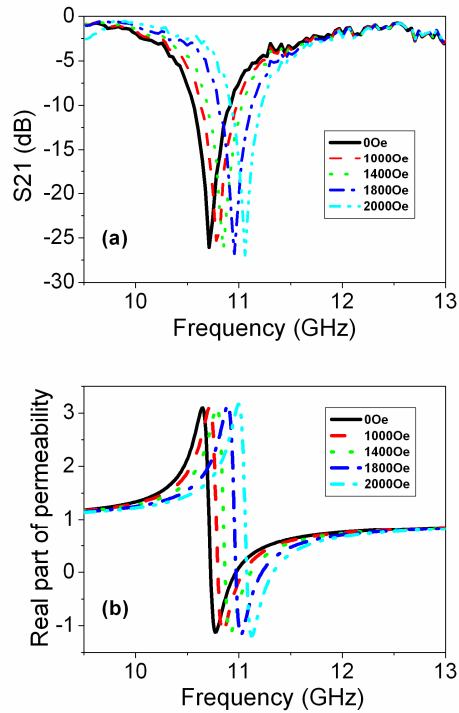


Fig. 4. (a) Experimental S21 parameters of NPM sample with dc magnetic field within the range of zero to 2000 Oe. (b) The dispersions of effective permeabilities of the NPM sample under corresponding dc magnetic field according to Eq. (1).

The inset of Fig. 1 and Fig. 4(b) respectively illustrate the calculated effective permeabilities of the sole NPM and those of the sample with YIG rods introduced under magnetic fields ranging from 0 to 2000 Oe. The lower red line in the inset of Fig. 1 shows that the effective permeability is negative in the range of 11.24–11.48 GHz for the sole NPM. While in Fig. 4(b), after the introduction of YIG rods, the resonance frequency redshifts due to the increase of ambient effective permittivity. And accordingly, the negative effective permeability occurs at 10.73–10.97 GHz. As the applied dc magnetic field increases, compared to that of the zero field, the resonance frequency keeps on shifting to higher frequency, with the negative effective permeability occurring at 10.80–11.04 GHz for  $H_0=1000$  Oe and 11.08–11.33 GHz for  $H_0=2000$  Oe.

To draw a brief conclusion from Fig. 4, with YIG rods introduced and magnetic field properly applied, a negative effective permeability could be achieved within the frequency range of 10.73–11.33 GHz and this range is widened by about 360 MHz compared to that of none YIG rods.

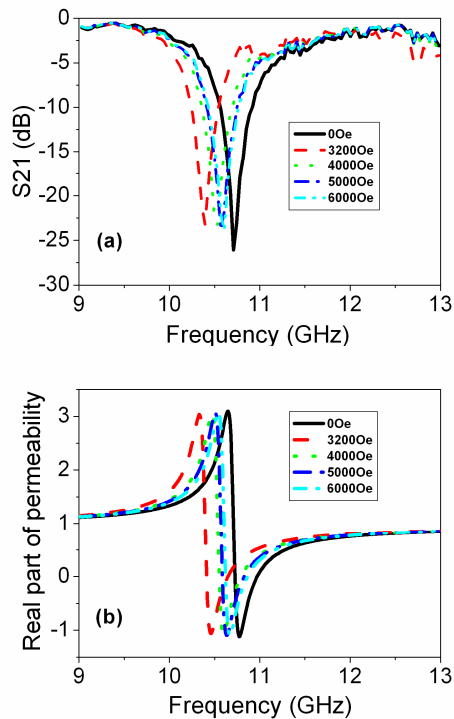


Fig. 5. (a) Experimental S21 parameters of NPM sample with dc magnetic field within the range of 3200 to 6000 Oe. (b) The dispersions of effective permeabilities of the NPM sample under corresponding dc magnetic field according to Eq. (1).

What Fig. 5 demonstrates is the tuning resonances of NPM sample under “high” magnetic field within the range of 3200 Oe to 6000 Oe. The plot of zero magnetic field is also shown for the comparison. It can be seen in Fig. 5(a) that, for  $H_0=3200$  Oe, NPM resonates at a relatively low frequency of 10.40 GHz compared to that for zero field, which is attributed to the corresponding large value of  $\mu_{1x}$  shown in regime 3 of Fig. 2. Indicated also by this regime is the decrease of  $\mu_{1x}$  with decreasing slope from values higher than unity, which causes the resonance frequency of the NPM to continuously blueshift with a gradually decreasing rate. A further indication is that, we could continue to neglect the influence of  $\mu_{2x}$ , with this approximation supported by the similarity between the S21 parameters of magnetic field in this range and that of zero field. Similar to Fig. 4(b), Fig. 5(b) shows the calculated effective permeabilities under magnetic fields ranging from 3200 to 6000 Oe, with the tunable negative effective permeability occurring at 10.42-10.86 GHz. This range is widened by about 200 MHz compared to that of none YIG rods. Additionally, the almost recovered S21 parameter of  $H_0=6000$  Oe back to that of  $H_0=0$  Oe accords well with the evolution of  $\bar{\mu}_{x,am}$  which decreases toward unity under high magnetic field as shown in regime 3 of Fig. 2. On the other hand, after removing the magnetic field, the resonance would immediately return to its original state, i.e., the shift is completely continuous and reversible.

Regarding the “medium” magnetic field between 2200 and 2800 Oe, Fig. 6(a) demonstrates a distinct tuning resonance of the NPM sample from those of Fig. 4 and Fig. 5.

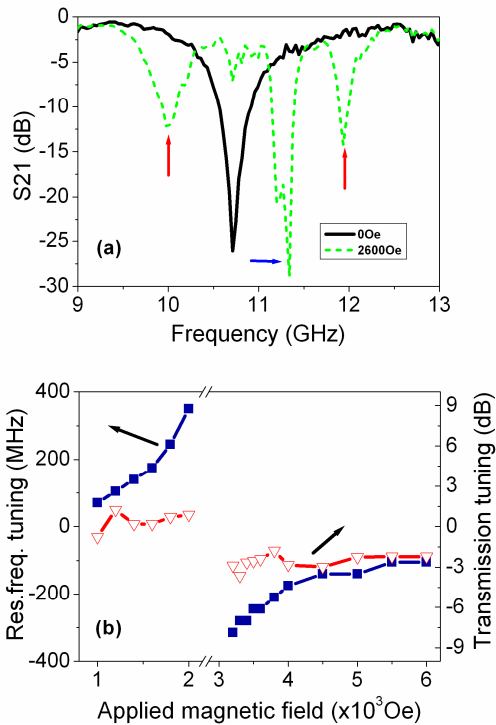


Fig. 6. (a) Experimental S21 parameters of NPM sample with the dc magnetic field of 2600 Oe. (b) Dependence of the resonance frequency (Res. freq) tuning and transmission tuning of the resonance dips on the applied magnetic field compared that of zero magnetic field.

For applied magnetic field between 2200 and 2800 Oe, as the evolution shows in regime 2 of Fig. 2, despite the stronger variation of  $\mu_{1x}$  which would lead to a more successful tuning of NPM in a broader frequency range, the imaginary part  $\mu_{2x}$  now is considerably large and it could not be ignored any more. Similar to Fig. 4(a) and Fig. 5(a), Fig. 6(a) shows the S21 parameter under  $H_0=2600$  Oe, where the red and blue arrows indicate the resonances rising from NPM and FMR, respectively. It should be noted that the resonance of NPM actually breaks down under the “medium” magnetic fields, indicating a damped resonance which negative effective permeability would not necessarily take place [21]. This could be resulted from the large value of  $\mu_{2x}$  and thus the correspondingly increased effective resistance of the equivalent LRC circuit of SRR, as discussed previously in section 1. On the other hand, the appearance of a pair NPM resonance indicated by the two red arrows is an interesting observation. It should be noted that, when FMR and NPM resonance emerge in the same frequency range, the interaction between the NPM and YIG rods would be rather complicated. We hereby propose a qualitative explanation of the appearance of the pair of NPM resonance as follows: SRR cells located along the boundaries of the array actually ‘sense’ different ambient effective permeability from those in the center, and the large absolute value of  $\mu_{1x}$  in this regime makes this difference more influential. In other words, it is considered to arise from the edge effects of the finite magnetic ambient.

With all the S21 parameter dips measured included, Fig. 6(b) briefly summarizes our experiment. It clearly shows the variation of the resonance frequency tuning from that of zero magnetic field with the dependence being the magnetic field. Compared to the approximate

10.71 GHz under zero field, the resonance frequency blueshifts acceleratedly with increasing magnetic field and reaches 350 MHz under  $H_0=2000$  Oe. Then with  $H_0=3200$  Oe, it redshifts 315 MHz compared to 10.71 GHz and again blueshifts deceleratedly when the magnetic field continuously increases. In both of the two processes, the variation of the transmission dips approximates to zero, i.e., the transmission property remains relatively stable on the whole, indicating the potential applicability of tuning by this method. On the other hand, both of the evolutions of the resonance frequency and transmission tuning curves provide convincing evidence for the validity of evolution of  $\bar{\mu}_{x,am}$  in Fig. 2. It should also be noted that the critical magnetic fields of regime 2 in Fig. 2 are slightly different from those in the experiments. It is considered as a result of the difference between the magnetic effective medium composed of air and YIG rods from that of single YIG rod on account of the interaction among the YIG rods [31].

Microwave ferrite shows dispersive permeability for right-circular polarization due to the excitation of FMR but non-dispersive permeability for left-circular one. Therefore, the transmission properties of microwave ferrite samples in rectangular waveguide would be nonreciprocal in general. Nevertheless, this nonreciprocal behavior could be avoided by symmetrically arranging ferrites in the waveguides with care [29]. In our experiment, as shown in Fig. 1, the SRRs and the corresponding YIG rods are arranged symmetrically with respect to the middle longitudinal section parallel to the short metal walls of the waveguide. Therefore, despite that the YIG rods in each of the two symmetric rows (with respect to the middle section) would show different permeabilities for forward and reverse propagating electromagnetic waves, the transmission of the sample as a whole should be reciprocal. The experimental S21 and S12 (not shown) parameters under certain dc magnetic field indicate the resonance of the NPM sample at the same frequency with almost the same amplitudes. The slightly nonreciprocal behavior is considered to be a result of the imperfect arrangement of the samples. Accordingly, it is safe to assume that negative effective permeabilities of NPM sample for forward and reverse propagating electromagnetic waves would emerge at the same frequency range with slightly different peak values.

#### 4. Conclusion

To conclude, we have proposed and experimentally demonstrated a magnetically tunable negative permeability metamaterial composed of a periodic array of SRRs and yttrium iron garnet ferrite rods. A qualitative explanation has also been suggested based on the effective-medium theory. With varied dc magnetic field, the resonance frequency of NPM could be dynamically tuned towards both higher and lower frequencies. Correspondingly, the negative effective permeability of NPM could be achieved within a large frequency range. This would inspire the design of active devices based on metamaterial such as the broadband cloak within the microwave and optical frequency domains as long as the appropriate magnetic material is selected.

#### Acknowledgments

This work is supported by the National Science Foundation of China under Grant Nos. 50425204, 50572043, 50632030, and 60608016, and by the Postdoctoral Science Foundation under Grant No. 20060390043.